Correlation between rheology and morphology of compatibilized immiscible blends

W. Gleinser*, H. Braun, Chr. Friedrich† and H.-J. Cantow
Freiburg Materials Research Center (FMF), and † Institut für Makromolekulare Chemie, Hermann-Staudinger-Haus, Albert-Ludwigs-Universität, Stefan-Meier-Strasse 31a, D-7800 Freiburg, Germany
(Received 24 December 1992; revised 22 March 1993)

The compatibilization effect of poly(styrene-*b*-methyl methacrylate) on the immiscible polymer blend of polystyrene and poly(styrene-*co*-acrylonitrile) was examined by dynamic mechanical spectroscopy. Special regard was taken of additional relaxation processes in the flow region, which were analysed using weighted relaxation-time spectra. Furthermore, an important topic of our research was the characterization of the morphology by energy-specific transmission electron microscopy. By increasing the amount of compatibilizer, the average particle size decreases from large polystyrene domains ($R \simeq 0.2\ \mu m$) down to micellar dimensions ($R \simeq 60$ nm). In this way, typical morphological structures in the blends were related with rheological behaviour. With a modified emulsion model from Choi and Schowalter, some correlations between particle size and trends in interfacial tension could be established dependent on compatibilizer concentration. Especially, it was found that the particle size reduction and the reduction of interfacial tension occur in different ranges of block-copolymer concentration.

(Keywords: compatibilized blends; rheology; morphology)

INTRODUCTION

Most polymers are immiscible, because of their small combinatorial entropy of mixing and the mostly positive enthalpy of mixing. Blending of immiscible polymers, however, is a simple method for combining advantageous properties of commercial polymers. But typically, in these macrophase-separated systems, the minor phase is dispersed in domains of about 0.5 to 10 μm. This structure is very sensitive to processing procedures, and it often causes problems, e.g. in mechanical properties or long-time behaviour of the final materials. The use of diblock copolymers as compatibilizers is one method to overcome these problems. Block copolymers increase the degree of dispersion, improve the adhesion between phases and stabilize the phases against coalescence. These effects are thought to go back to the decrease of interfacial tension if the compatibilizer occupies the interface. In the field of block-copolymer compatibilization of binary blends, three possible systems can be distinguished:

(i) A/A-*b*-B/B. Here the repeat units of the blend components and of each block of the copolymer, A and B, are identical[1–3]. This type of mixing is a thermodynamically athermal process. Several experimental investigations[4–7] have shown that the block molecular weight should be equal to or higher than that of the corresponding bulk polymer in order to exhibit good phase adhesion.

(ii) A/C-*b*-D/B. In this case, the blocks C and D of the block copolymer are chemically different from the corresponding polymers, A and B, in the bulk phases but thermodynamically miscible with them[8–10]. The resulting exothermic interaction enhances the compatibilizing effect of the block copolymer.

(iii) A/A-*b*-D/B. This is a combination of the above two possibilities, with one identical pair and one pair with exothermic interaction[11].

The investigations in this paper concern the A/A-*b*-D/B system. The immiscible blend system polystyrene (PS) and poly(styrene-*co*-acrylonitrile) (PSAN) was compatibilized with poly(styrene-*b*-methyl methacrylate) (P(S-*b*-MMA)). On the A/A side the molecular weight of the A block, M'_A, is nearly the same as that of the A polymer in the bulk phase, M_A, and therefore compatibilization should occur. This means that the block copolymer behaves just like an emulsifier in restraining phase separation of the homopolymers into their macroscopic domains. On the B/D side M_B is higher than M_D, but the thermodynamic driving force between the miscible polymer pair PSAN and PMMA[12] should overcome the restriction given by the molecular weights. For these cases, the tendency to form macroscopic block-copolymer phases with lamellar morphology is very small.

To characterize the efficiency of the compatibilizer, the flow behaviour of the blends was determined by dynamic mechanical spectroscopy to estimate the characteristic time constants. Furthermore, the morphology of the blends was studied by transmission electron microscopy to observe the dispersing effect of the block copolymer. With a modified emulsion model from Choi and Schowalter[13], we tried to correlate morphological

* To whom correspondence should be addressed

0032-3861/94/010128-08

structures and rheological behaviour. This model relates a characteristic relaxation time in the blend with the interfacial tension between the components and the size of dispersed particles.

In the next section, besides the materials used, the devices and measuring conditions are described. The results of dynamic mechanical spectroscopy and transmission electron microscopy are then presented, which is followed by the discussion of the results of the pure and the compatibilized blends.

EXPERIMENTAL

Materials

As matrix polymer, a technical poly(styrene-*co*-acrylonitrile) (PSAN) sample with a content of 20 wt% acrylonitrile (BASF AG) was used. The disperse phase was commercial polystyrene (PS) (BASF AG). The compatibilizer was an anionically synthesized symmetric diblock copolymer (P(S-*b*-MMA)) of polystyrene and poly(methyl methacrylate) (SM43)[14,15]. Details are listed in *Table 1*.

The blends were prepared by common precipitation of a solution in tetrahydrofuran (THF) (10 wt%) into methanol and dried in a vacuum oven for at least two days. For the investigations the compositions PSAN/SM43/PS = $70/x/30-x$ with $x=0$, 1, 1.8, 2.5, 5 and 10 by weight were chosen. For rheometry, the blends were pressed at 180°C under vacuum to discs with radius $r=12.5$ mm and thickness $h=1$ mm.

Dynamic mechanical spectroscopy

The dynamic moduli were obtained on a Rheometrics Mechanical Spectrometer RMS-800 with parallel-plate geometry ($r=12.5$ mm). Isothermal frequency sweeps were recorded between 133 and 223°C in steps of 10°C, with an accuracy of ± 0.5°C. A further increase of temperature was impossible because of the ceiling temperature of PMMA. For temperatures $T \leqslant 173$°C the frequency range was 100 to 10^{-2} rad s^{-1}, and for $T > 173$°C the range was extended to 10^{-3} rad s^{-1} to reach the terminal flow region. Above 173°C an inert N_2 atmosphere was used to suppress oxidation. The strain was kept below $\gamma = 0.3$ to stay within the linear viscoelastic regime, which was tested by strain sweeps. Master curves were constructed at a reference temperature $T_0 = 183$°C from the dynamic moduli G' and G''. The frequency sweeps were shifted without further corrections horizontally and vertically by a mathematical shift procedure[16]. For each blend, the relaxation-time spectrum from G' and G'' was calculated by a non-linear regularization method based on Tikhonov regularization[17].

Table 1 Characterization of the blend components

	M_w (10^3 g mol^{-1})[a]	M_w/M_n[a]	η_0 (Pa s)[c]
PSAN	205	1.62	9.10×10^5
PS	42[b]	1.03	5.75×10^2
SM43	81	1.12	–

[a] G.p.c., PS standard
[b] Additionally an impurity of about 4% with $M_w \simeq 3.4 \times 10^5$ g mol^{-1} was detected
[c] From dynamic measurements $T_0 = 183$°C

Creep experiments were carried out on a Rheometrics Stress Rheometer RSR to get highly deformed samples for subsequent morphology studies. All measurements were made with parallel-plate geometry ($r=12.5$ mm) at 160°C, inert N_2 atmosphere and constant stress command $\sigma = 50$ Pa. The samples were quenched during flow to a temperature below the glass transition in about 3 min while retaining the stress command on the sample and correcting the gap to avoid normal forces and therefore destruction of the morphology.

Transmission electron microscopy (TEM-ESI)

Ultrathin cuts of the quenched discs were obtained by a Leica Ultracut-E microtome with a diamond knife. The cuts were made at two positions: (i) in the middle of the disc ($r \simeq 0$), i.e. nearly non-deformation during the whole experiment, and (ii) at radius $r \simeq 10.5$ mm, i.e. nearly maximum of shear stress and deformation. The latter were examined in a radial and a tangential view through the samples, but are not shown in this paper. The ultrathin sections, thickness about 60 nm, were treated with RuO_4 vapour in order to increase contrast[18,19]. By this method, the PS domains are dark, the PSAN matrix is grey and the PMMA blocks are white on the photographs.

The TEM elastic bright-field images were taken on a Zeiss CEM 902, operated at 80 kV, with monoenergetic electrons (ESI mode). A 90 mm objective diaphragm was used corresponding to an 17.3 mrad aperture in back focal plane. Enlargements are indicated with labels in the images.

The average radius of the particles was determined by measuring in several typical photographs and calculating their arithmetical mean value.

RESULTS

Dynamic measurements

In *Figure 1* dynamic storage and loss moduli G' and G'' of the two blend components and the mixture PSAN/PS = 70/30 are plotted on different axes. In the plateau, transition and flow regions the curves of the blend components are typical for polymers with broad (PSAN) and narrow (PS) distributions[20]. The shoulder in the PS curve is caused by a high-molecular weight

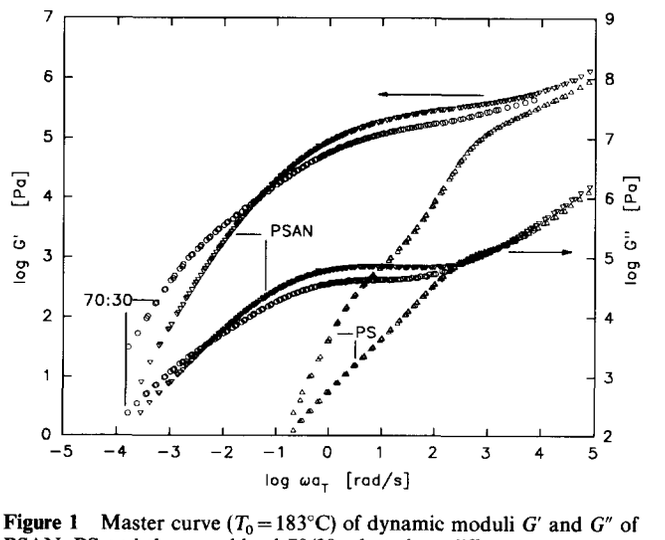

Figure 1 Master curve ($T_0 = 183$°C) of dynamic moduli G' and G'' of PSAN, PS and the pure blend 70/30: plotted on different axes

impurity in the technical product. The master curve of the blend shows a broad intermediate region between the plateau and the flow region. Furthermore, the flow region with $G' \propto \omega^2$ and $G'' \propto \omega$ begins at lower frequencies as in the matrix material. Such additional contributions of elasticity are also reported for other immiscible blends[21-24].

The rheological behaviour of SM43 is described elsewhere[25]. The phase-separated block copolymer SM43 reveals the well known low-frequency behaviour with $G' \propto \omega^{0.5}$ and $G'' \propto \omega^{0.5}$. Additionally, a significant shear influence on the morphology was observed.

The dependence of the dynamic moduli on the compatibilizer concentration is shown in *Figure 2*. For the sake of clarity only those compositions with $x=0$, 1.8, 5 and 10 are plotted. With an increasing amount of block copolymer the additional intermediate region found in the pure blend is changed in its extension, its height and its position on the frequency axis, but an exact characterization of the changes is impossible. For $x=10$ the terminal flow region could not be reached and further relaxations appear.

Transmission electron microscopy (TEM-ESI)

The morphologies of the blends with different amounts of block copolymer are shown in *Figures 3a* and *3f*. The ellipsoidal shape of the particles in the blends is caused by the cutting procedure. This was confirmed by rotating the cutting direction 90°. In the pure blend the average radius of the dispersed spheres (PS) is approximately $R \simeq 175$ nm. For $x=1$ and $x=1.8$ the particle size does not decrease remarkably, whereas for concentrations higher than 1.8% the PS domains decrease down to micellar dimensions (about $R \simeq 60$ nm). The radii of particles of all the blends are listed in *Table 2* and plotted in *Figure 6*.

DISCUSSION

Improved analysis by weighted relaxation-time spectra

In order to improve the analysis of the master curves, the relaxation-time spectra $H(\tau)$ were calculated and the weighted spectra $\tau H(\tau)$ were plotted against relaxation time τ. In *Figures 4* and *5* the plots corresponding to

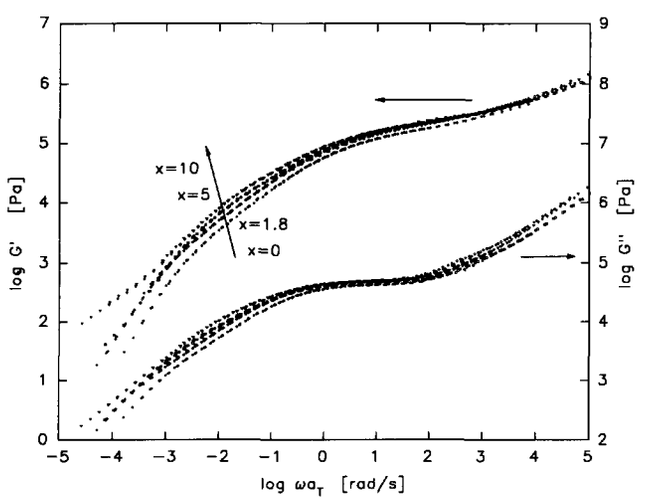

Figure 2 Master curve ($T_0=183$°C) of dynamic moduli G' and G'' of the blends PSAN/SM43/PS=70/x/30−x with $x=0$, 1.8, 5 and 10; plotted on different axes

Table 2 Blend properties dependent on compatibilizer concentration

SM43 (%)	η_b (Pa s)	τ_1 (s)	R (nm)	α (10^{-3} N m^{-1})
$x=0$	1.55×10^6	500	175	1.1
$x=1$	2.5×10^6	630/1580	157	0.8/0.3
$x=1.8$	3.0×10^6	1260	151	0.4
$x=2.5$	$\approx3.1\times10^6$	500	74	0.5
$x=5$	$\gg3\times10^6$	500	69	0.5
$x=10$	$\gg10^7$	400	51	0.4

Figures 1 and *2* are shown. By this method, the single processes can be separated.

For the PS sample, two narrow peaks can be seen (see insert in *Figure 4*) as expected from the moduli. The PSAN spectrum shows one broad peak due to the molecular-weight distribution. Compared with the spectra of the components, the spectrum of the pure blend shows an additional peak (the so-called mixing peak) at a longer relaxation time of $\tau_1=500$ s. This mixing peak is indicated in *Figure 4* by an arrow. In this way, the intermediate region in the master curve could be identified as a transition from the plateau zone of the PSAN to an additional relaxation process in the blend with the characteristic time constant $\tau_1=500$ s. The matrix spectrum appears as a shoulder on the mixing peak and is decreased because of lower volume fraction. The common point of intersection of the components and the blend (see insert) is a remarkable feature. This means that in this region the relaxation processes are nearly unaffected by each other and a simple additive mixing rule holds (see equation (8)).

In *Figure 5* the effect of compatibilizer is shown for all compositions. With 1% SM43 the mixture peak is split into two peaks. The first one appears nearly at the position of the mixing peak of the pure blend, the other one at a longer time $\tau_1=1580$ s. For $x=1.8$, the mixing peak of the pure blend disappears completely and one peak is left at $\tau_1=1260$ s. With an increasing amount of SM43 this peak of $x=1.8$ is now shifted back to shorter relaxation times and reaches a saturation value at $\tau_1 \simeq 500$ s. As expected, the weighted spectrum for $x=10$ increases strongly at longest relaxation times due to the high dynamic moduli for the lowest frequencies measured. The relaxation times represented by the maxima of the mixing peaks are listed in *Table 2* and are illustrated in *Figure 6* together with the particle radii R.

The most important fact is that τ_1 shows a maximum at $x=1$ and $x=1.8$, whereas R is decreased remarkably above a block-copolymer concentration of 1.8%. In the next two subsections the results of τ_1 and R are discussed in terms of a modified emulsion model from Choi and Schowalter[13] to understand the correlation between rheological behaviour and typical morphological structures.

The emulsion model for the pure blend

First of all, an emulsion model developed by Choi and Schowalter[13] is introduced for the case of the pure blend. The model was evaluated for non-dilute emulsions of deformable particles. Scholz *et al.*[24] applied this model to immiscible polypropylene/polyamide-6 (PP/PA6) blends and got a qualitative interpretation of their results. An application including a modified loss modulus was suggested by Gramespacher[21], who achieved

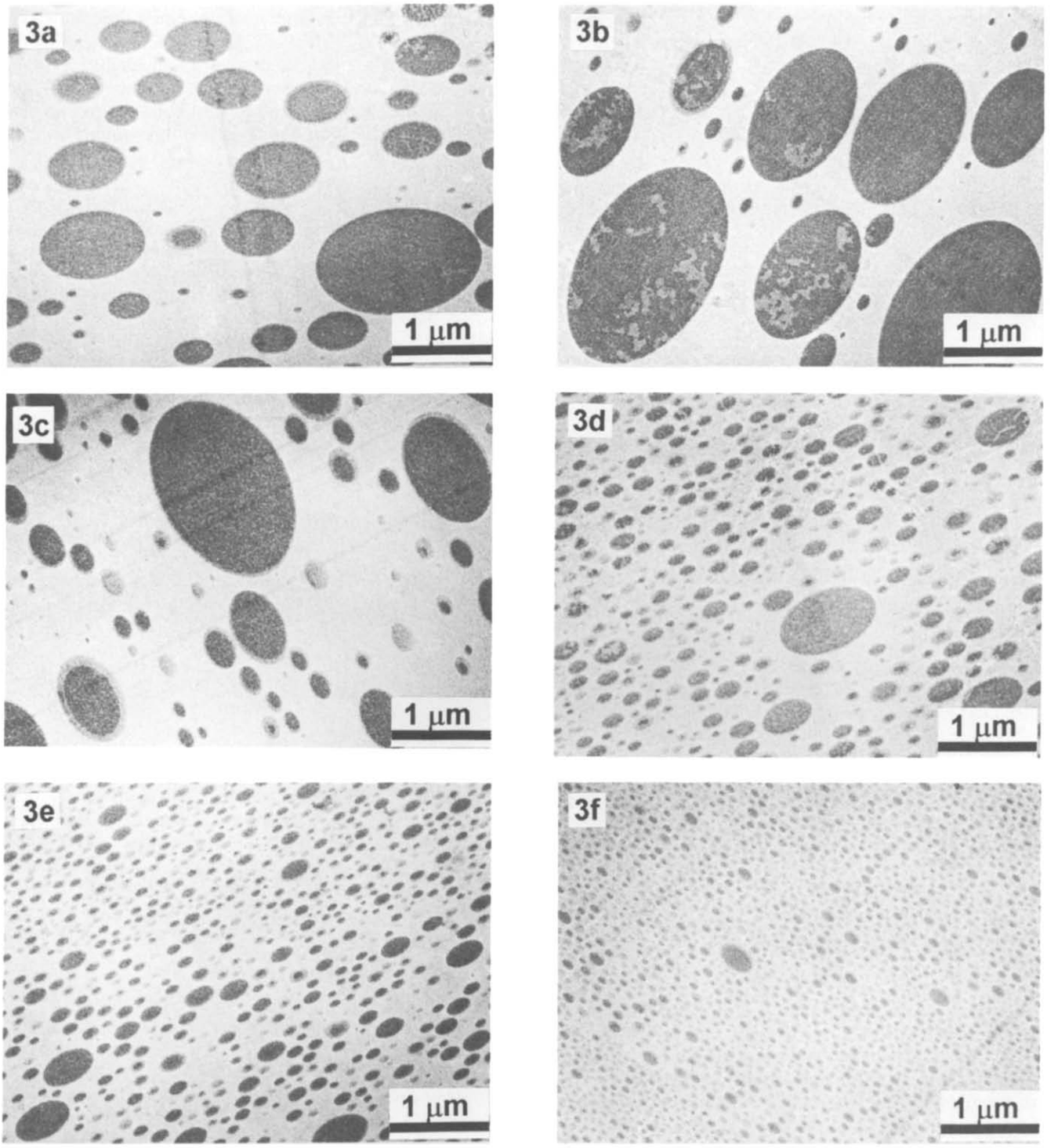

Figure 3 TEM photographs of the blends PSAN/SM43/PS = 70/x/30 − x with (a) x = 0, (b) x = 1, (c) x = 1.8, (d) x = 2.5, (e) x = 5 and (f) x = 10

a quantitative description of the experiments. We took his equations for the examination of our results:

$$G'(\omega)=\eta_b\frac{\omega^2(\tau_1-\tau_2)}{1+\omega^2\tau_1^2}=\frac{\eta_b}{\tau_1}\left(1-\frac{\tau_2}{\tau_1}\right)\frac{\omega^2\tau_1^2}{1+\omega^2\tau_1^2} \quad (1)$$

$$G''(\omega)=\frac{\eta_b}{\tau_1}\left(1-\frac{\tau_2}{\tau_1}\right)\frac{\omega\tau_1}{1+\omega^2\tau_1^2} \quad (2)$$

with

$$\eta_b=\eta_m\left(1+\phi\frac{(5k+2)}{2(k+1)}+\phi^2\frac{5(5k+2)^2}{8(k-1)^2}\right) \quad (3)$$

$$\tau_1=\tau_0\left(1+\phi\frac{5(19k+16)}{4(k+1)(2k+3)}\right) \quad (4)$$

$$\tau_2=\tau_0\left(1+\phi\frac{3(19k+16)}{4(k+1)(2k+3)}\right) \quad (5)$$

$$\tau_0=\frac{\eta_m R}{\alpha}\frac{(19k+16)(2k+3)}{40(k+1)} \quad (6)$$

In these equations, ϕ is the volume fraction of the dispersed phase and k is the viscosity of the dispersed phase (η_d) divided by the viscosity of the matrix material

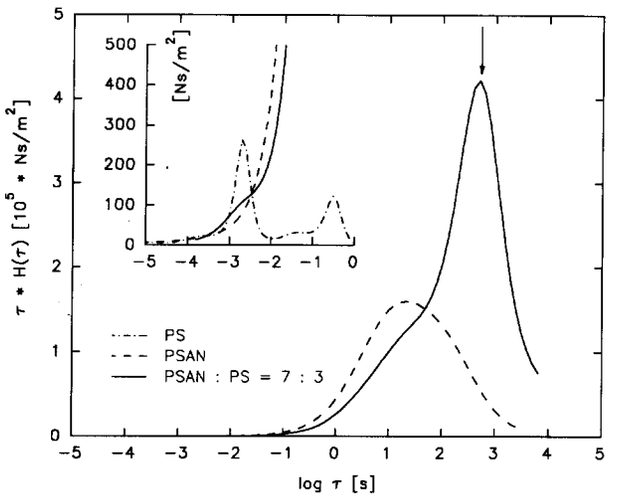

Figure 4 Weighted relaxation-time spectra ($T_0 = 183°C$) of PSAN, PS and the pure blend 70/30; calculated from G' and G''

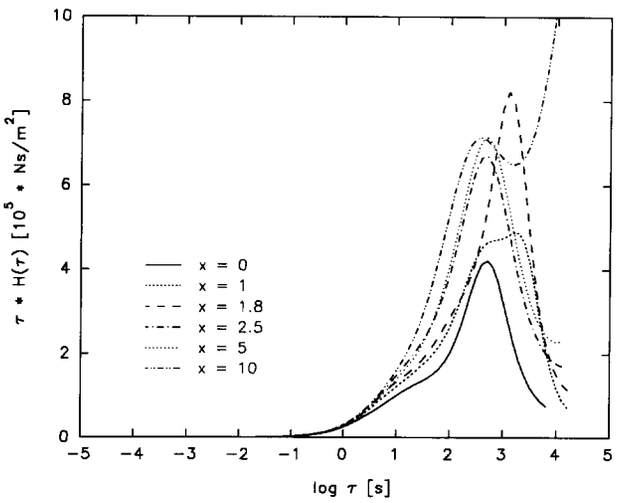

Figure 5 Weighted relaxation-time spectra ($T_0 = 183°C$) of the blends PSAN/SM43/PS = 70/x/30 − x = 0, 1, 1.8, 2.5, 5 and 10; calculated from G' and G''

(η_m). For viscoelastic fluids, η_m and η_d have to be represented by their zero-shear viscosities η_0 (see *Table 1*), because the model was evaluated for Newtonian liquids. Also, η_b is the blend viscosity calculated according to equation (3), R is the radius of the dispersed particles and α is the interfacial tension between the two blend components PS and PSAN.

With the parameters $\phi = 0.3$ and $k = 6.32 \times 10^{-4}$, the blend viscosity $\eta_b = 1.39 \times 10^6$ Pa s was calculated by equation (3). The value obtained is smaller than the experimentally determined viscosity of 1.55×10^6 Pa s (assessed from a Cole–Cole plot with $\eta'' \rightarrow 0$; see dotted curves in *Figure 7*).

After that, an improved approximation of equation (3) was used. The original equation from Choi and Schowalter[13] (equation (26)) was evaluated up to terms of order $O(\phi^{5/3})$ instead of $O(\phi)$. The result is:

$$\eta_{bn} = \eta_m \left(1 + \phi \frac{(5k+2)}{2(k+1)} + \phi^2 \frac{5(5k+2)^2}{8(k+1)^2} - \phi^{8/3} \frac{21k(5k+2)}{4(k+1)^2} + \phi^3 \frac{25(5k+2)^3}{32(k+1)^3} \right) \quad (7)$$

The value of the blend viscosity obtained from equation (7) is $\eta_{bn} = 1.54 \times 10^6$ Pa s and relates better to the experimental result; η_b and η_{bn} are indicated in *Figure 7* as filled diamonds on the η' axis.

In the next step we tried to simulate the experimental data by a calculation based on a simple mixing rule (cf. Gramespacher[21]):

$$G_b^* = \phi G_{PS}^* + (1-\phi) G_{PSAN}^* + G_i^* \quad (8)$$

In this equation G_b^*, G_{PS}^* and G_{PSAN}^* are the complex moduli of the blend and the individual components, and G_i^* is the complex modulus of the contribution caused by the interfacial tension in the phase-separated blend. G_i^* is defined by equations (1) and (2). The following parameters were used for the calculation of G_i^*:

$\eta_m = 9.10 \times 10^5$ Pa s	zero-shear viscosity of the matrix
$\eta_d = 5.75 \times 10^2$ Pa s	zero-shear viscosity of the dispersed phase
$k = 6.32 \times 10^{-4}$	the quotient $k = \eta_d/\eta_m$
$\eta_{bn} = 1.54 \times 10^6$ Pa s	blend viscosity calculated by equation (7)
$\phi = 0.3$	volume fraction of the dispersed phase
$\tau_1 = 500$ s	relaxation time determined from weighted relaxation-time spectrum (*Figure 4*)

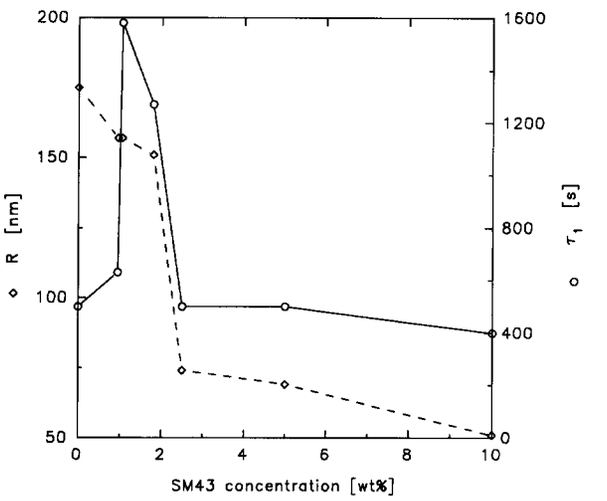

Figure 6 Particle radii and relaxation times of the blends PSAN/SM43/PS = 70/x/30 − x with x = 0, 1, 1.8, 2.5, 5 and 10

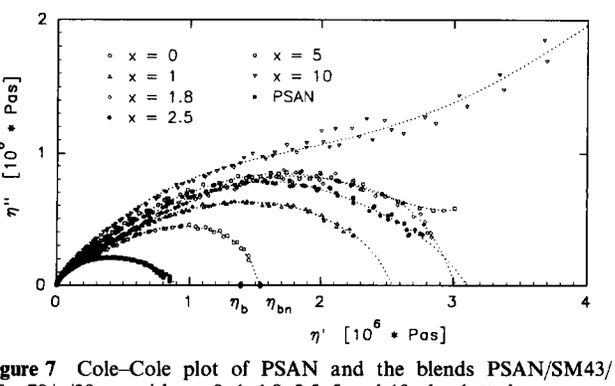

Figure 7 Cole–Cole plot of PSAN and the blends PSAN/SM43/PS = 70/x/30 − x with x = 0, 1, 1.8, 2.5, 5 and 10; the dotted curves are drawn to assess the blend viscosities. Calculated η_b and η_{bn} are indicated as filled diamonds on the η' axis

Figure 8 demonstrates that only a qualitative description of the experimental results is achieved. In the plateau zone the simple mixing rule works well, whereas the calculated curve is too low around τ_1 and in the terminal zone.

One reason for the failure in the mixing zone could be the high concentration of dispersed PS. Therefore, the distance between the particles becomes small and cooperative phenomena can take effect. Such phenomena are also discussed for other materials with a complex suprastructure[26]. They lead to an intermediate power-law region between plateau and terminal flow region as observed in the master curve of the blend (see *Figure 1*). But this behaviour is not taken into account by the model, which considers only hydrodynamic interactions between neighbouring particles.

Another reason could be the distribution of the particle sizes in the blend. Because of this distribution, according to the equations (4) and (6) not only one characteristic relaxation time but a corresponding distribution should be used for the calculation of G_i^*. Then the single Maxwell mode in G_i^* is replaced by multiple modes and it might be possible that an intermediate region (as seen in *Figure 1*) arises.

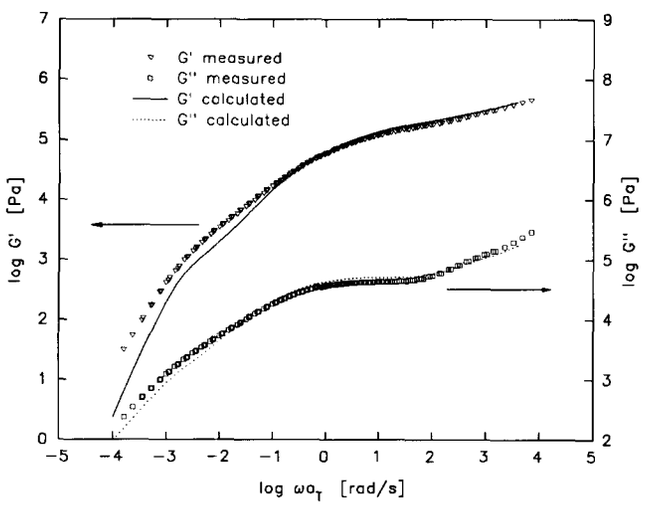

Figure 8 The experimental dynamic moduli G' and G'' of the pure blend 70/30 and the calculated data from the modified emulsion model of Choi and Schowalter[13]

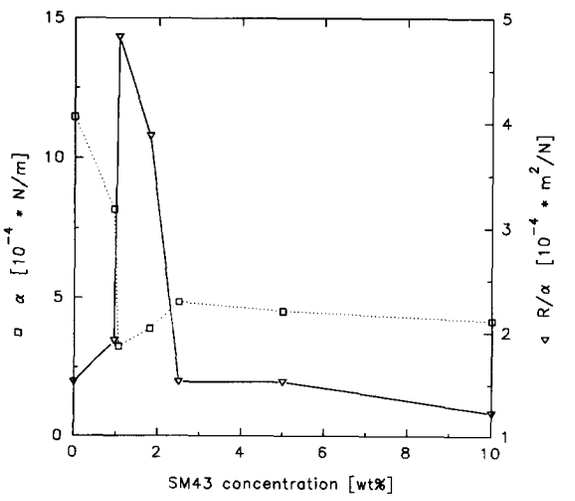

Figure 9 The quotient R/α and the calculated interfacial tension α of the blends PSAN/SM43/PS = 70/x/30 − x with x = 0, 1, 1.8, 2.5, 5 and 10

Consequently, a quantitative analysis of the experiments is not advisable, but a discussion of qualitative trends provides some interesting results for the blend without compatibilizer as well as for the compatibilized blends.

By equations (4) and (6) and τ_1 (τ_1 from the weighted spectrum) the quotient R/α is defined exactly. If either R or α is known, the other variable can be estimated. In this investigation, the size of the dispersed particles was measured by TEM as described in the 'Experimental' section. With the particle radius $R = 175$ nm for the pure blend the interfacial tension was ascertained with equations (4) and (6) as $\alpha = 1.1 \times 10^{-3}$ N m^{-1}. To the best of our knowledge, the interfacial tension of the system PS/PSAN has never been measured and published. However, the interfacial tension can be estimated approximately by the harmonic mean equation[27,28]. It yields $\alpha = 0.95 \times 10^{-3}$ N m^{-1} at $T = 180$°C as well as a very small temperature dependence of the interfacial tension ($\partial\alpha/\partial T = -1 \times 10^{-6}$ N m^{-1} K^{-1} for PS/PSAN in contrast to $\partial\alpha/\partial T \simeq -1 \times 10^{-5}$ N m^{-1} K^{-1} for other systems known from the literature[29]).

At this point of the paper some comments have to be made concerning the time–temperature superposition (TTS). Following the simple mixing rule in equation (8), at least one of the two criteria described below must be performed, so that a master curve can be created. On the one hand, if two of the moduli have nearly the same order of magnitude, they must have the same shift factors. On the other hand, if the shift behaviour is not identical, one of the two moduli must be much higher than the other.

In the plateau region ($\omega a_T > 10^2$ rad s^{-1}) the first case approximately holds for PS and PSAN (e.g. $T_0 = 183$°C and $T = 153$°C: $a_T^{PS} = 46$, $a_T^{PSAN} = 67$). For $\omega a_T < 10^2$ rad s^{-1} the modulus of PSAN matrix is much higher than that of PS and, concerning only these two contributions, a master curve can be created. However, in the region of the mixing peak ($\omega a_T < 10^{-2}$ rad s^{-1}) the contributions to the master curve caused by the interface (G_i^*) and the matrix (G_{PASN}^*) are of the same order of magnitude. Therefore both relaxation processes must show the same shift behaviour. The temperature dependence of the mixing peak is characterized by $\eta_b(T)$ and $\tau_1(T)$ (see equations (1) and (2)). With $\eta_b(T) = \eta_m(T) f_1(k(T), \phi)$ (see equation (3)) and $\tau_1(T) = \eta_m(T) f_2(\alpha(T), k(T), R, \phi)$ (see equations (4) and (6)), one can see that TTS should work well if f_1 and f_2 are independent of temperature. For small k values f_1 and f_2 are independent of variations in k, i.e. the temperature dependence of the zero-shear viscosities do not have to be equal. This means that f_1 is a constant and since α is almost independent of temperature, f_2 is also a constant. Therefore the mixing peak shows the identical shift behaviour as the matrix and a master curve is possible.

Compatibilized blends

Keeping in mind that only trends should be discussed, the emulsion model was also used to analyse the compatibilized blends, although it is not derived for this case. With an increasing amount of compatibilizer the experimental blend viscosity increases (see *Table 2* and *Figure 7*). This behaviour is not explained by equation (3) or (7) because η_b or η_{bn} is only dependent

on the constant parameters k, η_m and ϕ ($\phi = \phi_{PS} + \phi_{SM43}$). As already mentioned for the pure blend, there may be particles with short distances to each other. The modified interface with brushes on it enhances the interactions between such particles. These interactions may increase the blend viscosity. Similar observations were made for A/A-*b*-B systems with micellar morphology, where the overlapping of the micelles also leads to an increase of viscosity[30].

In contrast to the blend viscosity, the change in the relaxation times can be interpreted in principle by equations (4) and (6): the smaller the interfacial tension α and the greater the dispersed particles, the longer is the relaxation time for the corresponding mixing peak. By taking the radii of the dispersed particles (*Figures 3b–f* and *Table 2*) and the corresponding relaxation times τ_1, the interfacial tension for each concentration can be calculated due to the relation $\tau_1 \propto R/\alpha$. For $x = 1$ we used the two detected relaxation times and calculated with one particle radius two different interfacial tensions. In *Figure 9* the quotient R/α and the estimated interfacial tensions α are plotted *versus* compatibilizer concentration.

In *Figures 6* and *9* there are four main features:

(i) The examination of the TEM photographs shows a significant reduction of the particle size at $x = 2.5$.
(ii) The curve of τ_1 and R/α has a maximum at $x = 1$ and 1.8.
(iii) The interfacial tension α is completely reduced at $x = 1.8$.
(iv) The interfacial tension in the compatibilized blends is about three times smaller than in the pure blend. This magnitude of reduction is confirmed by other systems known from the literature[31].

The first and third of the points above show that the reduction of interfacial tension and particle size do not occur in the same range of concentration of compatibilizer. The non-simultaneous changes in R and α can be explained in the following way:

For $x = 1$ the estimated two interfacial tensions calculated from the doublet peak might indicate that at this low concentration not all the particles are compatibilized.

With 1.8% SM43 the whole interface is occupied (saturation at the interface) and the interfacial tension is decreased to its lowest value. At this concentration the particles are not decreased because a reduced particle size would result in more interfacial area than can be occupied. With this lowered interfacial tension and the nearly unchanged particle radius, τ_1 is longer than for the uncompatibilized blend.

If more compatibilizer is added during blend preparation (2.5%), the excess favours the formation of smaller particles in order to produce more interfacial area. Now the smaller particles with decreased interfacial tension have a shorter relaxation time τ_1. This means that one portion of the compatibilizer ($\simeq 1.5\%$) in each blend is used up for lowering the interfacial tension. The rest ($x - 1.5$) can then be used for particle size reduction.

For $x \geqslant 5$, the particles cannot be decreased further and additional compatibilizer may form micelles in the matrix or in the dispersed phase. Thermodynamic calculations[10] based on scaling concepts, TEM and the strongly increased viscosity for $x = 5$ and 10 indicate that the micelles are in the matrix.

SUMMARY AND CONCLUDING REMARKS

The analysis of the pure blend by the emulsion model of Choi and Schowalter[13] modified by Gramespacher[21] and the correction introduced here for higher concentrations showed that a qualitative description of the blend behaviour can be achieved for the system under consideration. The evaluation of η_b to terms of order $O(\phi^{5/3})$ yields an improved quantitative prediction for the blend viscosity. This is not the case for the contribution to the master curve caused by the interface. In order to test whether the failure is caused by the high content of minor phase, some blends with $0.05 < \phi < 0.3$ should be analysed. In order to examine the influence of the particle size distribution on the rheological behaviour, the distribution function has to be determined from the TEM photographs and taken into account in the model. Nevertheless, the interfacial tension determined was in good agreement with the prediction from the harmonic mean equation.

This emulsion model was also applied to compatibilized blends. By this application correlations between changes in morphology and rheological time constants dependent on compatibilizer concentration were found. The reduction of interfacial tension and the reduction of particle size do not occur simultaneously. A first portion of compatibilizer is used up for decreasing the interfacial tension to a lowest value (three times smaller with 1.8% compatibilizer) and then surplus block copolymer reduces the size of the dispersed particles (at $x \geqslant 2.5$). Beyond this concentration the effects at the interface are completed and further comptibilizer may form micelles in the blend. Further examinations with compatibilizer concentrations between $x = 0$ and 2.5 have to be made to verify the non-simultaneous behaviour in this range.

Additionally to this, block copolymers with lower molecular weights should be used to suppress the increase of the blend viscosities observed even at low compatibilizer concentration. Then, on the A side of the A/A-*b*-D/B system the PS should be replaced by a polymer miscible with PS, so that the thermodynamic driving force overcomes the restriction given by the low molecular weight of the block copolymer as is the case for the pair PMMA/PSAN.

ACKNOWLEDGEMENTS

We gratefully acknowledge financial support by Bundesministerium für Forschung und Technologie, BMFT, and BASF AG. We thank Dr C. Auschra (University of Mainz) for supplying us with the block copolymer and J. Weese for making it possible for us to calculate the relaxation-time spectra.

REFERENCES

1 Fayt, R., Jêrome, R. and Teyssié, Ph. *J. Polym. Sci., Polym. Phys. Edn.* 1982, **20**, 2209
2 Wippler, C. *Polym. Bull.* 1991, **25**, 357
3 Löwenhaupt, B. and Hellmann, G. P. *Colloid Polym. Sci.* 1990, **268**, 885
4 Riess, G., Kohler, J., Tournut, C. and Bandert, A. *Makromol. Chem.* 1967, **101**, 58
5 Inoue, T., Soen, T., Hashimoto, T. and Kawai, H. *Macromolecules* 1970, **3**, 87
6 Meier, D. J. *Polym. Prepr.* 1977, **18**, 340
7 Xie, H., Liu, Y., Jiang, M. and Yu. T. *Polymer* 1986, **27**, 1928
8 Won Ho Jo, Ho Cheol Kim and Doo Hyun Baik *Macromolecules* 1991, **24**, 2231

9 Ouhadi, T., Fayt, R., Jerôme, R. and Teyssié, Ph. *J. Polym. Sci., Polym. Chem. Edn.* 1986, **24**, 973
10 Braun, H., Rudolf, B. and Cantow, H. J. *Makromol. Chem., Theory Simul.* 1993, submitted
11 Ouhadi, T., Fayt, R., Jérôme, R. and Teyssié, Ph. *Polym. Commun.* 1986, **27**, 212
12 Fowler, M. E., Barlow, J. W. and Paul, D. R. *Polymer* 1987, **28**, 1177
13 Choi, S. J. and Schowalter, W. R. *Phys. Fluids* 1975, **18**, 420
14 Allen, R. D., Smith, S. D., Long, T. E. and McGrath, J. E. *Polym. Prepr.* 1985, **26** (1), 247
15 Auschra, C., Stadler, R. and Voigt-Martin, I. G. *Polymer* 1993, **34**, 94, 2081
16 Honerkamp, J. and Weese, J. *Rheol. Acta* 1993, **32**, 57
17 Honerkamp, J. and Weese, J. *Rheol. Acta* 1993, **32**, 65
18 Trent, J. S., Scheinbeim, J. I. and Couchman, P. R. *Macromolecules* 1983, **16**, 589
19 Montezinos, D., Wells, B. G. and Burns, J. L. *J. Polym. Sci., Polym. Chem. Edn.* 1985, **23**, 421
20 Ferry, J. D. 'Viscoelastic Properties of Polymers' 3rd Edn., Wiley Interscience, New York, 1980, p. 391
21 Gramespacher, H. and Meissner, J. *J. Rheol.* 1992, **36**, 1127
22 Valenza, A., Lyngaae-Jørgensen, J., Utracki, L. A. and Sammut, P. *Polym. Networks Blends* 1991, **1**, 79
23 Graebling, D. and Muller, R. *J. Rheol.* 1990, **34**, 193
24 Scholz, P., Froelich, D. and Muller, R. *J. Rheol.* 1989, **33**, 481
25 Braun, H., Gleinser, W. and Cantow, H.-J. *J. Appl. Polym. Sci.* 1993, **49**, 487
26 Friedrich, Chr. *Phil. Mag. Lett.* 1992, **66**, 287
27 Wu, S. *J. Polym. Sci. (C)* 1971, **34**, 19
28 Hobbs, S. Y., Dekkers, M. E. J. and Watkins, V. H. *Polymer* 1988, **29**, 1598
29 Wu, S. 'Polymer Interface and Adhesion', Marcel Dekker, New York, 1982, p. 112
30 Watanabe, H. and Kotaka, T. *Macromolecules* 1984, **17**, 342
31 Patterson, H. T., Hu, K. H. and Grindstaff, T. H. *J. Polym. Sci. (C)* 1971, **34**, 31